npj | climate and atmospheric science

Article

Published in partnership with CECCR at King Abdulaziz University

https://doi.org/10.1038/s41612-024-00624-2

Future drought risk and adaptation of pastoralism in Eurasian rangelands

Banzragch Nandintsetseg[1,2,7] ✉, Jinfeng Chang[3,7] ✉, Omer L. Sen[1], Christopher P. O. Reyer[4], Kaman Kong[5], Omer Yetemen[1], Philippe Ciais[6] & Jamts Davaadalai[2]

Drought risk threatens pastoralism in rangelands, which are already under strain from climatic and socioeconomic changes. We examine the future drought risk (2031–2060 and 2071–2100) to rangeland productivity across Eurasia (West, Central, and East Asia) using a well-tested process-based ecosystem model and projections of five climate models under three shared socioeconomic pathway (SSP) scenarios of low (SSP1−2.6), medium (SSP3−7.0), and high (SSP5−8.5) warming relative to 1985–2014. We employ a probabilistic approach, with risk defined as the expected productivity loss induced by the probability of hazardous droughts (determined by a precipitation-based index) and vulnerability (the response of rangeland productivity to hazardous droughts). Drought risk and vulnerability are projected to increase in magnitude and area across Eurasian rangelands, with greater increases in 2071–2100 under the medium and high warming scenarios than in 2031–2060. Increasing risk in West Asia is caused by longer and more intense droughts and vulnerability, whereas higher risk in Central and East Asia is mainly associated with increased vulnerability, indicating overall risk is higher where vulnerability increases. These findings suggest that future droughts may exacerbate livestock feed shortages and negatively impact pastoralism. The results have practical implications for rangeland management that should be adapted to the ecological and socioeconomic contexts of the different countries in the region. Existing traditional ecological knowledge can be promoted to adapt to drought risk and embedded in a wider set of adaptation measures involving management improvements, social transformations, capacity building, and policy reforms addressing multiple stakeholders.

Rangelands represent the world's largest biome, occupying more than 40% of the total land surface[1]. They provide critical ecosystem services[2,3], such as biodiversity, carbon sequestration, and animal feed[2,4], and are hence central for food security and the livelihoods of people, particularly of rural populations in climate-sensitive drylands, such as Eurasia, where livelihoods are heavily reliant on natural resources, including pastoralism[4–8]. The Eurasian drylands (Fig. 1a) comprise the world's largest contiguous rangelands[1], with low and variable (intra- and inter-annual) precipitation levels along with sparse vegetation, which has been grazed by livestock of mobile pastoralists for millennia[6,9]. In 2019, the Eurasian rangelands (EAR) hosted approximately 426.8 million head of livestock (equal to 835.1 million in sheep units)[10], fed either directly by grazing or indirectly by grass harvest. Rangeland ecosystems are the most sensitive to climate change, and rangeland grazing has been precisely tuned to match high climate variability[11–14]. For millennia, the traditional ecological knowledge of pastoralists[15,16] has enabled them to manage the variations in climate (e.g., droughts) and forage production, including rotation and mobility of herds[17–19]. In recent decades, the mobility of pastoralists has been influenced by climate hazards, pasture and forage availability, and socioeconomic pressure, resulting in higher herd mobility and longer travel distances in search of favorable pastures and reduced mobility[18–20].

[1]Eurasia Institute of Earth Sciences, Istanbul Technical University, 34469 Istanbul, Türkiye. [2]ERDEM Research and Communication Center, 13312 Ulaanbaatar, Mongolia. [3]College of Environmental and Resource Sciences, Zhejiang University, Hangzhou, China. [4]Potsdam Institute for Climate Impact Research (PIK), Member of the Leibniz Association, 14412 Potsdam, Germany. [5]RIKEN Center for Computational Science, Kobe, Japan. [6]Laboratoire des Sciences du Climat et de l'Environnement, CEA-CNRS-UVSQ, Gif Sur Yvette, France. [7]These authors contributed equally: Banzragch Nandintsetseg, Jinfeng Chang.
✉e-mail: nandiad98@gmail.com; changjf@zju.edu.cn

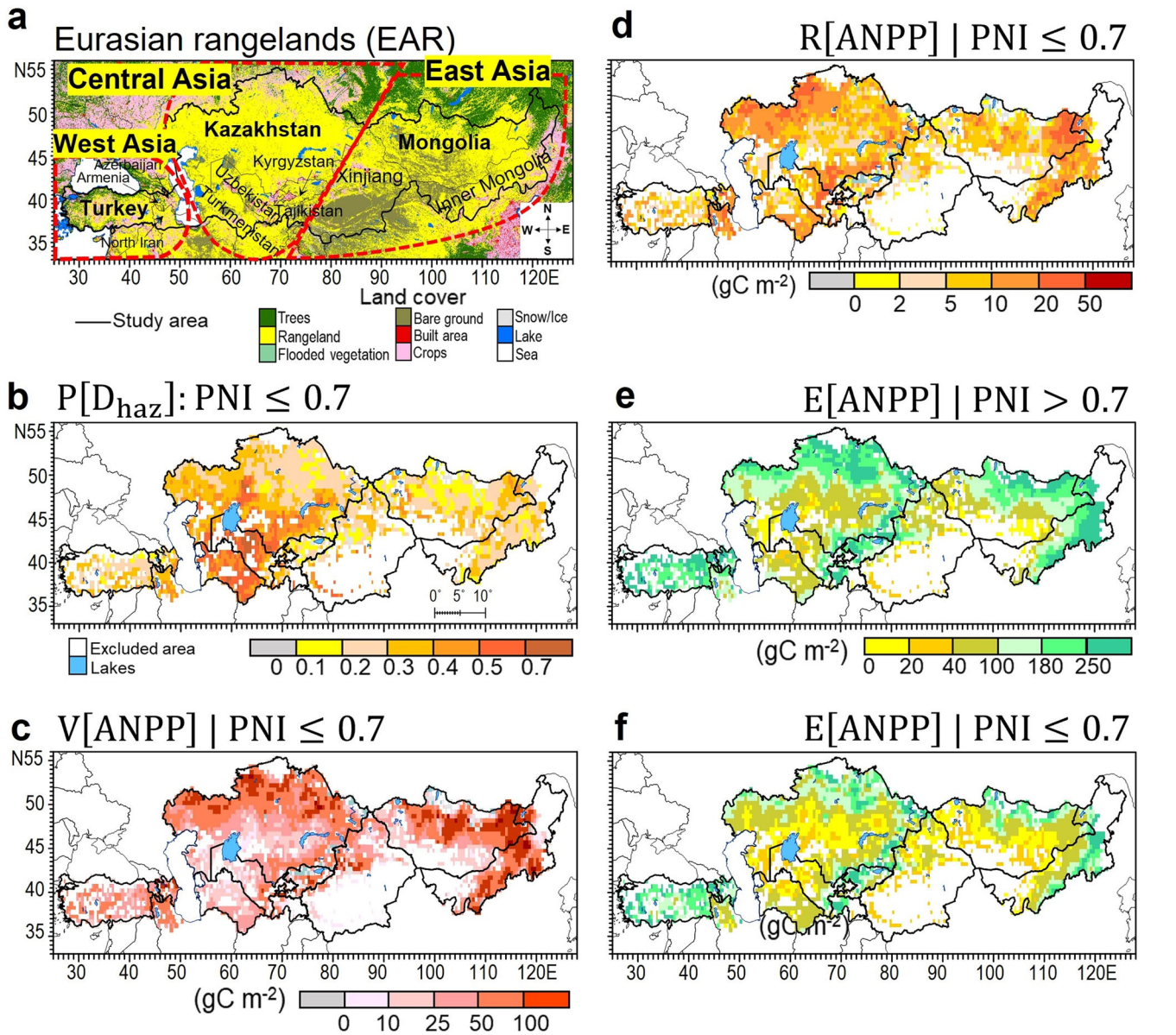

Fig. 1 | Probabilistic risk analysis (PRA) of the rangeland productivity (ANPP) over the EAR during the baseline period (1985–2014). **a** Study area (black solid line) including West Asia, Central Asia, and East Asia (dashed red lines). **b** Probability of hazardous droughts ($P[D_{haz}]$) for PNI ≤0.7 (moderate to severe). **c**, Vulnerability of the ANPP (difference between **e** and **f**). **d** Risk to the ANPP (multiplication of **b** and **c**). **e**, **f** ANPP in normal and nonhazardous drought years (favorable conditions) and in hazardous drought years (unfavorable conditions). The ANPP simulations by ORCHIDEE-GM are forced by the observed climate (GSWP3-W5E5). **b** The gray cells denote areas with normal conditions (e.g., PNI >0.7 for the whole period), and these areas are excluded from vulnerability and risk analyses (gray in **d**, **e**).

In recent decades, the EAR has experienced frequent droughts[13,21–23] and increased land-use pressure (such as overgrazing)[24,25] following economic and sociopolitical changes in countries in the EAR. During the transition phase (the 1990s), the livestock number significantly decreased, but it has rapidly increased in the last two decades, resulting in vegetation productivity loss[13,26–28] and rangeland degradation[25,29,30]. This, in turn, has jeopardized the viability of pastoralist livelihoods and food security, resulting in vulnerable herders who directly rely on rangeland production[17,31,32]. For instance, in the 2000s, frequent droughts, together with severe winters, led to pasture unavailability and inaccessibility, and killed ~30.2 million head of livestock (equal to 57.4 million sheep units) in Mongolia[24]. Drought-induced reduction of vegetation productivity decreases livestock body fat, leads to continuous loss of adequate grazing, and also, prevents pastoralists from gathering adequate forage for winter feeding. Both factors increase livestock mortality in winter due to starvation[31,32]. These climate shocks have caused socioeconomic damage to both pastoralists and the entire nation[31], resulting in poverty, food insecurity, unemployment, malnutrition, and health, driving pastoralists to migrate from rural to urban areas in search of alternative livelihoods[33–37]. Following the above shocks, the number of pastoralists has decreased year by year, with an end to herding and outmigration[33,35] (also referred to as climate or environmental migration), threatening the future sustainability of pastoralism.

Droughts are anticipated to become more frequent and intense in the future[38,39] and may pose challenges in achieving several of the United Nations Sustainable Development Goals (in particular, SDG1—no poverty, SDG2—zero hunger, SDG3—good health and well-being, and SDG15—life on land) in the region[40]. The sixth assessment report of the Intergovernmental Panel on Climate Change (IPCC AR6)[39] highlighted that there is only limited evidence on the projected future impact of climate change on

livestock production, particularly in low- to medium-income countries, and that more robust and detailed information on the risk and vulnerability of rangelands is needed[41]. Understanding the drought risk to rangeland productivity is crucial for developing adaptation and conservation strategies to ensure pastoralism sustainability. However, compared to other regions, substantial uncertainty remains regarding the future drought impacts on the EAR, and detailed regional analyses are missing.

Risk terminology was developed under the auspices of the United Nations[42] and used by the IPCC[41,43] for studying human systems and for ecosystem risk[44–46] by explicitly distinguishing hazard, vulnerability, and risk. Risk is defined as the expected loss and calculated as the product of hazard and vulnerability. Hazard is the probability of occurrence of a potentially damaging phenomenon. Vulnerability is the resultant degree of loss upon phenomenon occurrence[42]. Understanding the drought risk to the rangeland productivity in the EAR under future climate change is of utmost importance for ensuring sustainable pastoralism in the region, which is becoming increasingly unstable[33,34] due to climatic[23,31] and socioeconomic[31,32] changes. However, there is a lack of regional-level assessment studies of future drought impact on the EAR and the associated risks for decision-makers as well as adaptation measures to manage future risks based on climate change scenarios. Here, we applied an ecosystem-focused probabilistic risk analysis (PRA) method[45,46] to assess the future changes in the drought risk (impacts) to rangeland productivity across the EAR (Fig. 1a). Furthermore, we synthesized the main adaptation measures for pastoralism in the EAR from a wide range of literature sources (Supplementary Table 1) and assessed which key stakeholders they target and whether they address the drought risk or vulnerability as outlined by our PRA approach. In this study, we use the terms "hazardous drought", "drought risk", and "vulnerability". Hazardous drought is the probability of hazardous (moderate to severe) drought occurrence ($P[D_{haz}]$) representing a potentially damaging phenomenon. Drought risk (R) refers to the risk to rangeland productivity, which is defined as the expected loss of the rangeland productivity and can be calculated as the product of $P[D_{haz}]$ and the vulnerability (V) of rangeland productivity to hazardous droughts. Vulnerability can be calculated from the response of the rangeland productivity (i.e., the aboveground net primary productivity, *hereafter* referred to as productivity) simulated by the process-based ecosystem model Organizing Carbon and Hydrology in Dynamic Ecosystems–Grassland Management version 3.2 (ORCHIDEE-GM v3.2)[47,48]. $P[D_{haz}]$ can be calculated from the precipitation-based Percent of Normal Index (PNI)[49] for the growing season (April−September). Hazardous droughts occur for PNI ≤0.7 (moderate to severe droughts) (refer to Methods). Here, we examined the changes in $P[D_{haz}]$, vulnerability, and risk over the EAR in two future time slices, namely, the mid- (2031–2060) and late- (2071–2100) 21st centuries, under three scenarios (SSP1–2.6, SSP3–7.0, and SSP5–8.5) relative to the baseline period (1985–2014). We obtained PRA using two climate datasets of observations (GSWP3-W5E5[50,51], 1901−2019) and downscaled and bias-corrected simulations (historical: 1971−2014 and future: 2015−2100) by five general circulation models (GCMs)[52] of the Coupled Model Intercomparison Project Phase 6 (CMIP6). The analysis was performed over three regions of the EAR (West Asia, Central Asia, and East Asia) (Fig. 1a), which are loosely divided considering mainly the geographical conditions, climate, and vegetation cover (Refer to Methods) across eleven countries (Mongolia, Kazakhstan, Kyrgyzstan, Tajikistan, Uzbekistan, Turkmenistan, Azerbaijan, Armenia, Turkey, North of Iran, and two provinces of China: Inner Mongolia and Xinjiang) in the spatial domains of 33°−56°N and 25°−128°E (Supplementary Fig. 1).

Results

Historical drought risk to rangeland productivity

In the baseline period (1985−2014), we examined the drought risk to the productivity across the EAR by applying the PRA method using the modeled productivity derived from ORCHIDEE-GM and the drought index represented by the PNI from the observation-based climate dataset (GSWP3-W5E5) (Fig. 1) and the five GCM simulations over the historical period (Supplementary Fig. 2). The PRA results driven by the observation-based climate and historical climate of the five GCMs exhibited similar spatial patterns of $P[D_{haz}]$, vulnerability, and risk (Fig. 1b–d versus Supplementary Fig. 2a–c) and consistent regional variations (Supplementary Fig. 3). The vulnerability increased from south to north in the EAR, while $P[D_{haz}]$ was higher in the southern regions of the EAR ($P[D_{haz}]$ >0.5 in southern Central Asian countries). Central Asia (40.2 ± 16.7% (±spatial standard deviation); notably northern Kazakhstan) and East Asia (49.7±19.9%; particularly central to eastern Mongolia and northern Inner Mongolia) showed higher vulnerabilities than West Asia (23.9 ± 15.2%) (Supplementary Fig. 3b and Supplementary Table 2). These results are consistent with those of previous studies reporting a higher vulnerability of productivity in Central Asia (particularly northern Kazakhstan)[28] and East Asia (northern Mongolia)[13]. The relative drought risk to productivity was higher in Central Asia (9.6 ± 5.9%) and East Asia (7.8 ± 5.3%) than in West Asia (4.4 ± 4.2%) (Supplementary Fig. 3c and Supplementary Table 2). The risk of hazardous droughts to productivity was the highest in the northern EAR (northwestern Kazakhstan, northeastern Mongolia, and northern Inner Mongolia), mainly due to the high vulnerability to exceptional droughts. The high risk in southern Kazakhstan and Uzbekistan is, however, mainly due to the high frequency of droughts. Additionally, we examined the alternative PRA method using $P[D_{haz}]$ based on soil moisture (soil moisture percentile[53], $W_p \leq 0.2$ (moderate to exceptional droughts, Supplementary Fig. 4) and standardized precipitation evapotranspiration[54] (SPEI ≤−1.0, Supplementary Fig. 5) drought indices. For baseline period, a parallel analysis using the alternative indicators of W_p or SPEI (Supplementary Figs. 4, 5) revealed that in general, the vulnerability and risk of hazardous droughts to productivity showed similar spatial patterns to those using the PNI as a drought indicator (Fig. 1). An exception was found in northern Kazakhstan and central Mongolia, where $P[D_{haz}]$ defined by W_p (Supplementary Fig. 4a) and SPEI (Supplementary Fig. 5a) was slightly higher than $P[D_{haz}]$ defined by the PNI (Fig. 1b). This further demonstrates that the PNI can be used to assess drought conditions. For the future period, the SPEI-based results revealed that hazardous droughts could occur every year in some grid cells, which, by definition, prevents calculating the vulnerability of productivity (and risk). The SPEI from the GCM climate projections (averaged proportion across GCMs) indicates that for 2031–2060 and 2071–2100, 1.8 and 2.7% (SSP1–2.6), 3.1 and 9.4% (SSP3–7.0), and 3.6 and 10.9% (SSP5–8.5) of the area over EAR will experience drought every year (i.e., SPEI <−1.0 for all 30 years in the future periods in those grid cells). Therefore, in the PRA for the future period, the PNI-based assessment was used because it does not have this conceptual problem.

Projected hazardous droughts under future climate change

The GCM projections show a significant future increase in the growing season air temperature (T_{4-9}) across the EAR under all three future climate scenarios relative to the baseline period (1985–2014) (Fig. 2a). T_{4-9} changes of a similar magnitude are projected across the three regions. Warming begins to decrease and stabilize under SSP1−2.6 after 2050, with magnitudes varying between 1 °C and 3 °C. Stronger warming is projected under the SSP3−7.0 and SSP5−8.5 scenarios with increases of +2.36–2.67 °C in 2031–2060 and increases of +4.80–6.12 °C in 2071−2100 relative to the baseline period. Differences in the magnitude of the temperature changes are found across the five GCMs (Fig. 2b and Supplementary Fig. 6a).

The projected changes in the growing season precipitation (P_{4-9}) under the three climate scenarios are shown in Fig. 2c, d. Slight changes in P_{4-9} are projected under the SSP1−2.6 scenario across the various regions. Under the medium and high warming scenarios (SSP3−7.0 and SSP5−8.5), divergent trends in P_{4-9} are found in the different regions, with a drying trend in West Asia (−5.9 to −14.6%), no change in Central Asia (0.5–3.5%) and a slight increasing trend in East Asia (1.1–12.7%) (Fig. 2d). This is consistent with regional and global studies based on the CMIP6 with declining precipitation in parts of the Mediterranean region (including West Asia)[55,56] and slight positive anomalies across land areas in Eurasia under

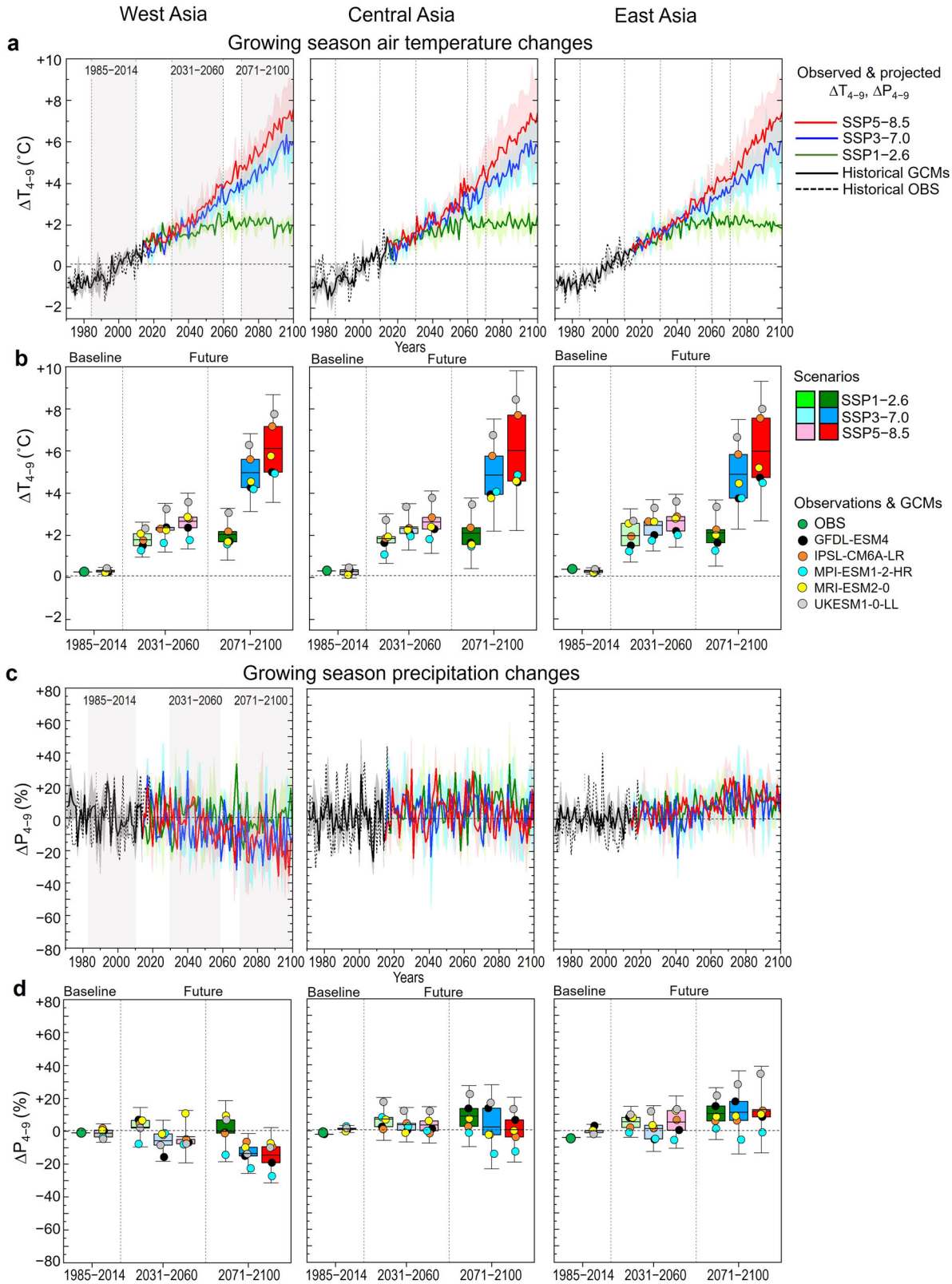

Fig. 2 | Growing season (April−September) surface air temperature (T_{4-9}) and precipitation (P_{4-9}) anomalies during 1971−2100 under the three scenarios by the five GCMs. The baseline period ranges from 1985 to 2014. **a**, **c** Regionally averaged ensemble time series showing the mean (solid lines) and interquartile range calculated across all models (colored shading). Anomalies from the observations (OBS) are denoted as GSWP3-W5E5 (1971−2019). The light gray shadings indicate 1985−2014, 2031−2060, and 2071−2100, the time periods used for construction of the boxplots and jitter plots. **b**, **d** Boxplots and jitter plots of the mean anomalies of the observations and five GCMs under each SSP scenario. The boxplots indicate the 25−75th percentile (box), with two standard deviations (whiskers), and mean values (line) of the estimated values for each period. The colored dots show the averaged values of each GCM.

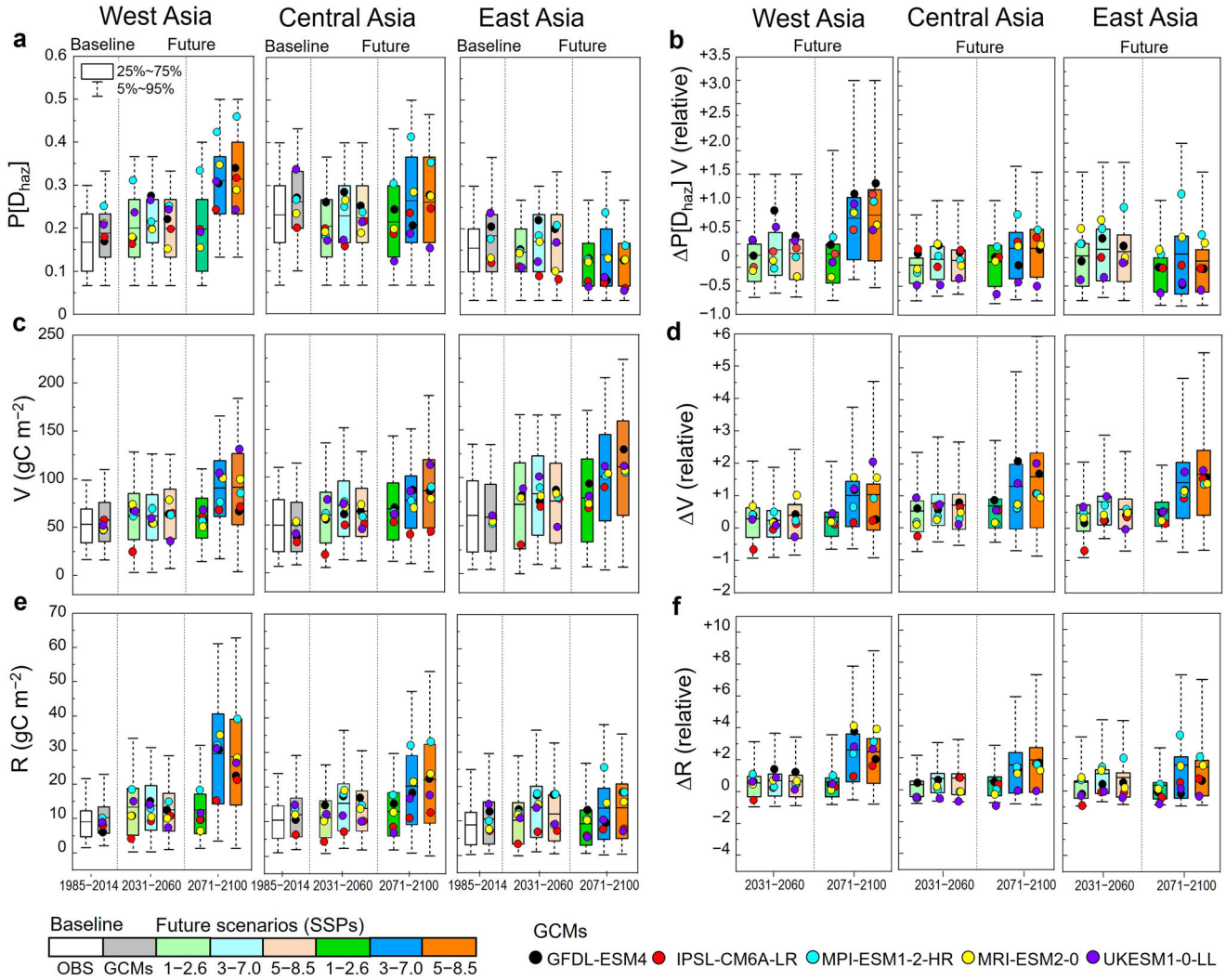

Fig. 3 | Future changes in the vulnerability (V) and risk (R) of the productivity (ANPP) to hazardous droughts ($P[D_{haz}]$) for the three regions. a–c Boxplots of V and R of the ANPP to hazardous droughts over the baseline (1985−2014) and future (2031−2060 and 2071−2100) periods under each SSP scenario. **d–f** Respective future changes (Δ, in relative terms) in $P[D_{haz}]$ ($\Delta P[D_{haz}]$), V (ΔV), and R (ΔR) during the future periods under each SSP scenario relative to the baseline. Each boxplot includes all values forced by the observations (OBS) of GSWP3-W5E5 and GCMs of all grid cells in each region. The boxplots indicate the 25−75th percentile (box) and 5−95th percentile (whiskers) and mean values (line) of the estimated values for each period. The colored dots show the averaged values of each GCM.

SSP5−8.5[55,57]. However, we found high variabilities in the precipitation projections over time and space across the five GCMs (Fig. 2d and Supplementary Fig. 6b).

The future changes in $P[D_{haz}]$ relative to the baseline period revealed diverse $\Delta P[D_{haz}]$ values (Fig. 3a, Supplementary Fig. 7, and Supplementary Tables 2, 3), as well as the corresponding duration and intensity (Supplementary Fig. 8), across the EAR for each GCM and scenario. At the regional level, no significant changes in the frequency, duration, and intensity of hazardous droughts are projected under the SSP1−2.6 scenario (low-warming scenario). However, under the medium and high warming scenarios, increases in the frequency, duration, and intensity of droughts are projected across the EAR (Fig. 3b, Supplementary Fig. 8, and Supplementary Table 2). All five GCMs consistently projected an increase in $P[D_{haz}]$ in West Asia (27 ± 39% for 2031–2060 and 27 ± 112% for 2071–2100) (Supplementary Table 3) relative to the baseline period with a longer duration and higher intensity. In Central Asia and East Asia, with increasing duration and intensity, the GCMs projected divergent changes in $P[D_{haz}]$, where $\Delta P[D_{haz}]$ is projected to increase in the projections of a few GCMs and to decrease in other GCM projections (Supplementary Fig. 7). Our findings are consistent with those obtained in recent studies based on the standardized precipitation drought index showing an increase in droughts in West Asia[58] and western Central Asia[55], and a slight decrease in the drought frequency in East Asia, including East Asian countries[57].

Projected drought risk to rangeland productivity

The vulnerability of productivity (expressed as $ANPP_{non\text{-}haz} - ANPP_{haz}$) to hazardous droughts was consistently projected to increase over the EAR by 43.3 ± 161%–61.3 ± 152% (ensemble mean ΔV) for 2031−2060 and by 54.0 ± 156%–143.5 ± 281% for 2071−2100 under the three scenarios, particularly under the medium and high warming scenarios (>57.3 ± 170% for 2031−2060 and >123.8 ± 237% for 2071−2100) (Fig. 3d and Supplementary Table 2). The differences in the spatial pattern of the changes in vulnerability are significant (Supplementary Fig. 9). The increasing vulnerability of productivity can be explained by the following two factors: i) a general increase in productivity (>24.1% across the various scenarios and regions) in the future in the nonhazardous drought years (i.e., higher $ANPP_{non\text{-}haz}$; Supplementary Fig. 10), and ii) the increase in the drought duration and intensity (Supplementary Fig. 11) tends to reduce the ANPP in drought years (i.e., lower $ANPP_{haz}$).

Under all scenarios, the future drought risk to productivity is projected to increase over the EAR during both periods (ensemble mean ΔR > 47.5 ± 246%), with more pronounced risk increases under the medium and

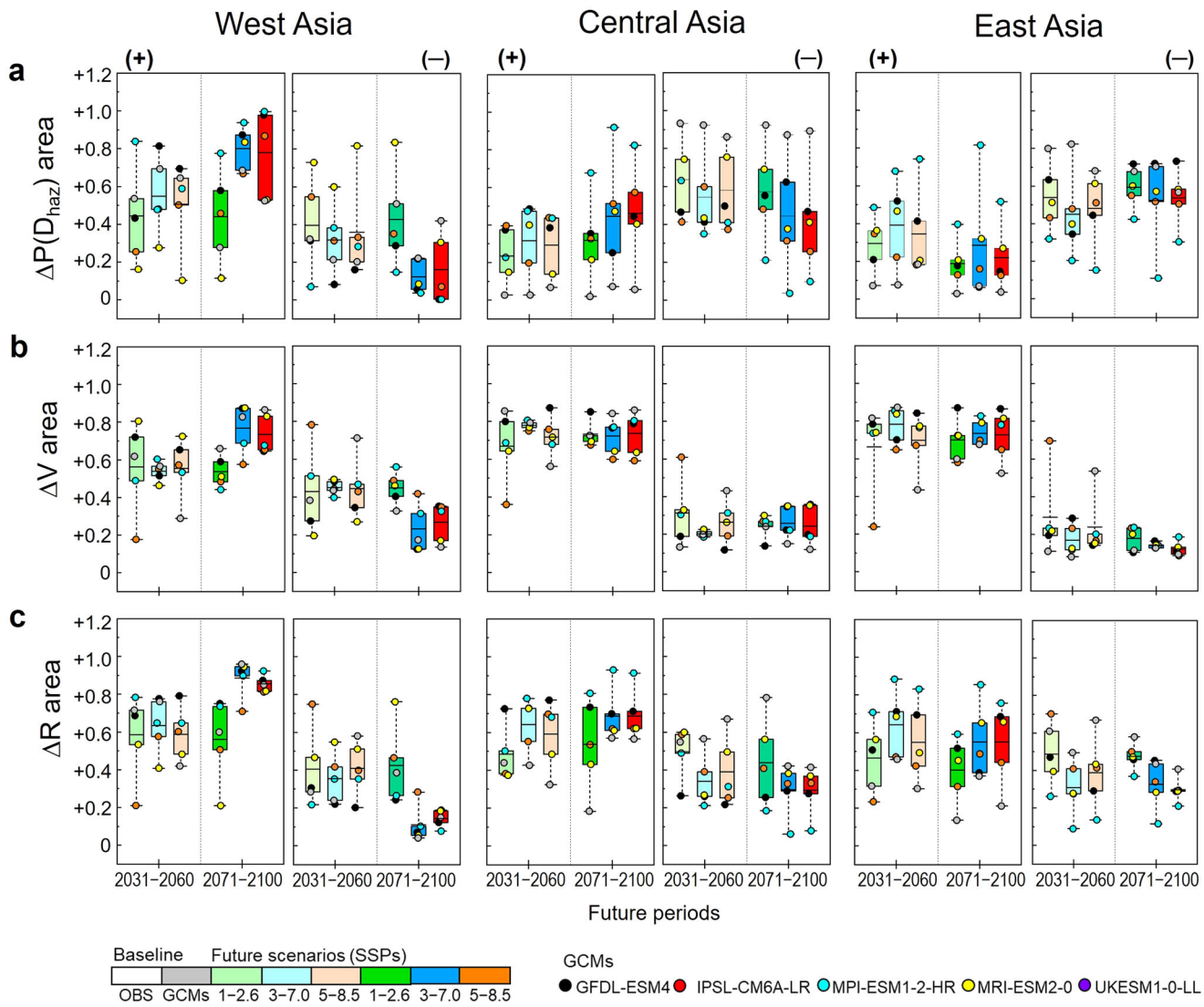

Fig. 4 | Future changes in the area of hazardous drought ($\Delta P[D_{haz}]$ area), vulnerability (ΔV area), and risk (ΔR area) to ANPP for the three regions. Areas in each region with increasing (+) or decreasing (−) values of **a** $\Delta P[D_{haz}]$ area, **b** ΔV area, and **c** ΔR area to the ANPP in 2031−2060 and 2071−2100 under all SSP scenarios relative to the baseline period (1985−2014): West Asia, Central Asia, and East Asia. The values are spatially averaged over cells in each region and each model (colored dots). The boxplots indicate the 25−75th percentile (box) and 5−95th percentile (whiskers) of the estimated values for each period.

high warming scenarios during 2071−2100 than in 2031−2060 (Fig. 3f and Supplementary Table 2). The spatial pattern of the changes in risk varies across the individual GCMs (Supplementary Fig. 12 and Supplementary Table 3). A consistent increase in the risk of productivity loss is projected under all scenarios in southwestern Central Asia (i.e., western Kazakhstan, Turkmenistan, and Uzbekistan across all GCMs) and northern East Asia (i.e., Mongolia, as indicated by the results of most GCMs, except UKESM1-0-LL; Supplementary Fig. 12). The largest increase in the risk of rangeland productivity loss is obtained under the medium and high warming scenarios in 2071−2100 (>74.8 ± 288% under SSP3−7.0 and SSP5−8.5) (Fig. 3f and Supplementary Table 2). In West Asia, the main cause for the attained risk increase (>65.2 ± 202% under SSP3−7.0 and SSP5−8.5) is the increase in both $P[D_{haz}]$, which has a longer duration and higher intensity, and the vulnerability of the EAR. In contrast, the increasing risks in Central Asia (>71.8 ± 262% under SSP3−7.0 and SSP5−8.5) and East Asia (>84.2 ± 291%) are associated with the increasing vulnerability rather than changes in $P[D_{haz}]$, indicating that vegetation is becoming more vulnerable to droughts.

To account for the spatial extent due to the changes in the drought frequency, vulnerability, and risk to productivity, we assessed the percentage of the areas in each region with increasing (+) or decreasing (−) drought frequency ($\Delta P[D_{haz}]$ area), vulnerability (ΔV area), and risk (ΔR area) values for 2031−2060 and 2071−2100 under all scenarios relative to the baseline period (1985–2014) (Fig. 4). During 2031−2060, similar area percentages in West Asia showed increases and decreases in $P[D_{haz}]$ across the various SSPs. However, by 2071−2100, a larger portion of the area (~80% on average across the GCMs) will experience increases in $P[D_{haz}]$, with the majority of grid cells showing positive $\Delta P[D_{haz}]$ values (Figs. 4a, 5a). In Central and East Asia across all GCMs, the areas with decreased $P[D_{haz}]$ and increased $P[D_{haz}]$ values are comparable, with a slightly larger area showing decreasing $P[D_{haz}]$ values (Fig. 3a). Regarding the changes in vulnerability, most areas of the EAR (over 60% on average across the GCMs) are projected to experience an increase in the drought vulnerability of rangeland productivity under all SSPs (Figs. 4b, 5b). As a result, a larger area is projected to experience an increased drought risk to rangeland productivity (Figs. 4c, 5c). Our results indicate that a future higher risk of simultaneous stronger rangeland productivity shocks is evident across a wider extent in the EAR. Stronger production shocks can be indicated by ΔV, while a wider extent can be observed in Figs. 4b, 5b.

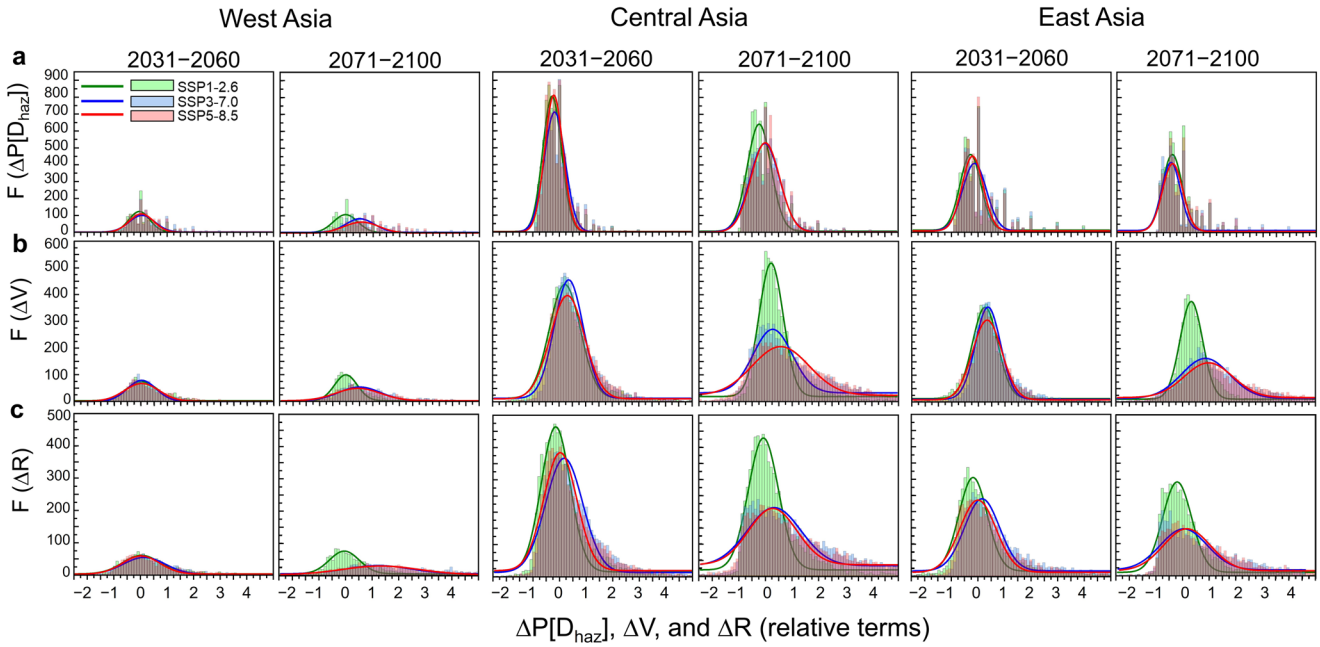

Fig. 5 | Future changes in frequency distribution of vulnerability and risk of ANPP to hazardous droughts in three regions. Distribution of the frequency (grid cells) of **a** hazardous droughts F(ΔP[D_{haz}]), **b** vulnerability F(ΔV), and **c** risk F(ΔR) of the ANPP for 2031−2060 and 2071−2100 under all SSP scenarios relative to the baseline (1985−2014) for West Asia, Central Asia, and East Asia. Each bin includes all values of the five GCMs for all grid cells in each region. The lines indicate the distribution curve of each SSP scenario.

Discussion

We found that the drought risk to rangeland productivity is projected to increase in magnitude and spatial extent across the EAR during the mid- and late-21st centuries under the medium and high warming scenarios. The higher risk in West Asia is associated with both the increasing frequency of hazardous droughts (with an increased duration and intensity) and vulnerability of rangelands, whereas the higher risks in Central Asia and East Asia are more closely related to the increased rangeland vulnerability (Fig. 3). Increases in the vulnerability of productivity, i.e., a larger productivity difference between normal and dry years, were projected in most areas across the EAR, particularly under the higher warming scenarios (SSP3−7.0 and SSP5−8.5; Figs. 3, 4, respectively) in 2071−2100. The increase in productivity in normal years (as simulated by ORCHIDEE-GM) can be partially attributed to the elevated atmospheric carbon dioxide (CO_2) levels. The latter often enhances plant photosynthesis and productivity, improves water use efficiency[59], and has the potential to mitigate soil moisture deficits. This effect might be more pronounced at high CO_2 concentrations[60] and might partially alleviate the impacts of higher temperatures and low precipitation levels (low PNI values). However, since the PNI is a simple precipitation-based drought index, further analysis of the potentially reduced drought frequency caused by elevated atmospheric CO_2 levels is not possible but has already been studied elsewhere[61]. In addition, elevated atmospheric CO_2 levels were recently found to result in lower net primary productivity levels in wet years than in dry years[62] caused by a changing species composition under elevated CO_2 levels and/or nutrient leaching[62], both of which are effects not included in the version of ORCHIDEE-GM used in this study. However, the performance of ORCHIDEE-GM in simulating the rangeland productivity and soil moisture has been validated against in situ observations and remote sensing products over European[47,63], Mongolian[13], and global grasslands[64,65] and further validated over the EAR in this study (Supplementary Fig. 13). Further model development should include the species composition or trait shifts and nutrient cycling to better address the above effects. The increase in the vulnerability of productivity can also result from the lower ANPP projected in dry years due to the more intense and longer droughts found during the future period (Supplementary Fig. 8).

The ecosystem-focused PRA[46] conducted in this study allows for straightforward quantification and decomposition of the risks of rangeland ecosystems. PRA analysis is based on probability distributions that represent both the temporal variability of drought and rangeland productivity. The occurrence of hazardous events is probabilistically expressed based on the frequency (i.e., P[D_{haz}]), while the impacts of the intensity and duration of drought events are implicitly accounted for in the productivity simulations by the process-based ecosystem model ORCHIDEE-GM. The simulated productivity decreases more under the influence of severe and longer droughts (Supplementary Fig. 11). However, we acknowledge that temporary interruptions of ecosystem activity due to shorter-duration droughts were not included in our risk analysis, given that a growing season PNI_{4-9} value of ≤0.7 was used in this study to identify hazardous drought years. The interaction between the environment and ecosystems is complex. Process-based models such as ORCHIDEE-GM could be used to simulate productivity reduction resulting from water stress caused by short-term droughts, while they can hardly account for vegetation adaptation to drought through a changing species composition and/or physiological adaptation[48]. Furthermore, vegetation can recover from drought and show resilience. Given the limitation of the PRA methodology, the sensitivity of hazardous drought on productivity (i.e., the vulnerability of productivity to drought) was assessed in this study, while resilience was not explicitly considered. However, it should be noted that the dynamic reserve carbon pool simulated in the process-based model allows regrowth after disturbances under suitable climate conditions. Such a process may partly account for vegetation recovery. Nevertheless, our PRA in this study is a major step in risk assessment over the EAR, and a detailed representation of vegetation resilience and species/community adaptation relies on an in-depth understanding of their interactions and quantification. We chose two 30-year time periods (2031–2060 and 2071–2100) to represent the mid- and

late- 21st century, whose 30-year timespan (long term) represents the average condition of climate because climate change is characterized in terms of a 30-year average. However, the 30-year average has limitations. For example, the averaging does not differentiate between consecutive hazardous years and hazardous years being spread out across the 30-year period, although the effects of several drought years happening in a row might be different from the effects of drought years with interspersed non-drought years.

Our findings also highlight significant uncertainties in regional estimates and spatial patterns. This is mainly attributed to the diverse climate changes projected across the EAR by the different GCMs (Supplementary Fig. 6). For example, UKESM1-0-LL projected a substantial increase in precipitation over Central Asia and East Asia, leading to a slight decrease in droughts in the future (Supplementary Fig. 7), which differs from the projections of the other GCMs. Nevertheless, utilizing climate projections derived from multiple GCMs allowed us to assess the possible range of future changes in the regional vulnerability and risk of rangeland productivity to hazardous droughts across the EAR. However, the simulated productivity is also uncertain because it is derived solely from ORCHIDEE-GM. Considering the potentially different sensitivities of the modeled productivity and associated carbon fluxes to climate change[66,67], a multi-model ensemble modeling approach could be used to further quantify the uncertainties related to the ecosystem model structure in the future.

Despite these uncertainties, it is evident that the EAR will face an increasing drought frequency (in particular in West Asia), higher vulnerability, and higher risk (Fig. 3) in a wider area of the region (Figs. 4, 5). Therefore, the adaptation of pastoralism to climate change is crucial to support the livelihoods of the local population. Pastoralism in Eurasian drylands has a long (mobile pastoralism) history[9,17,68], and the existing traditional ecological knowledge of how to tolerate the variation in forage production induced by the high seasonality and interannual variability of climate could serve as a valuable starting point for designing adaptation measures[15,18,19]. The traditional ecological knowledge (or indigenous and local knowledge) of pastoralists[15,19] to mitigate these variations includes hay and fodder storage, herd mobility adjustment, livestock and resource diversity, and reciprocity through pasture sharing, mutual assistance, and knowledge sharing (Table 1). However, in recent decades, the ability of pastoralists to manage drought and climatic shocks has been further challenged by continued environmental[31,32], political, and socioeconomic marginalization[20,29]. Thus, even though pastoralists have tolerated a highly variable climate in the past (Figs. 1a, 2), the challenges of adapting to future hazardous droughts (Fig. 3a) (with a longer duration and higher intensity, as shown in Supplementary Fig. 8) under climate change will increase because of this reduction in the adaptive capacity and because the magnitude and pace of climate change will most likely surpass the levels based on the long-standing traditional ecological knowledge of pastoralists. Thus, more frequent or severe forage shortages for local livestock, as shown by the increasing vulnerability and risk (Fig. 3b, c, respectively), could lead to livestock losses in the following winters, as historically observed in Mongolia[24,31] and Kazakhstan[6]. There is strong evidence that drought-related factors (lack of pasture availability, weak animals, and forage/hay reserve deficit) caused 35.0% of the observed 30.2 million livestock deaths in 2000–2014[24,31,32].

Given the increasing insecurity of pastoralism in Eurasian drylands[29,33,34], anticipating changes under future warming[39] and understanding future changes in the drought risk to rangeland productivity are critical for a broad suite of climate-sensitive pastoralism systems[8]. In addition to encouraging traditional ecological knowledge and associated adaptation measures, further adaptation to increasing drought vulnerability and risk to rangeland productivity within a changing socioeconomic context is urgently needed to support sustainable pastoralism and local livelihoods. To address this challenge and complement existing traditional ecological knowledge, evidence and recognition have increased that not only pasture management practices should be adapted. Additionally, it is crucial to foster adaptation at other levels of societal organization. Promoting institutions and improving governance to support policy reforms, capacity building, and social transformations could establish the underlying conditions for adaptation to occur within a wider sustainability context. Building upon our modeling results and document analysis, including scientific articles, reports from development banks, and international organizations (Supplementary Table 1), we compiled and synthesized the main pastoralism adaptation measures for three regions of the EAR (Table 1) and assessed whether they address the drought risk or vulnerability and who the key stakeholders are (policy-makers, government agencies, pastoralists, research institutions, and researchers, international organizations and other social and economic actors). While many of the proposed adaptation measures build on existing traditional ecological knowledge, such as reserves, rotational grazing, herd movement to allow rehabilitation, adjustment of herd numbers, and protection of emergency pastures, there is a wide range of strategies for improving adaptation through management improvement (including nature-based solutions such as increasing hay harvesting (fencing, fertilizing, seeding, and irrigation) and planting of more drought-tolerant forage species), social transformation, capacity building, and policy reform efforts (Table 1).

Management improvement measures include enhancing rangeland protection and restoration by rotational grazing, matching stocking rates with the rangeland capacity, promoting drought-tolerant livestock breeds, and increasing feed reserves. Measures related to social transformations include diversification of livelihoods, providing access to markets, and fostering cooperation within communities (to encourage the next generation of herders, as observed in most countries), while capacity-building measures highlight the need to establish monitoring systems to assess the vulnerability to drought, as well as improve knowledge sharing and transfer, e.g., with regard to the use of early-warning systems and other risk management tools. All EAR countries could focus on these measures. Moreover, these adaptation measures must be accompanied by policy reforms that improve infrastructure, transportation, information, technology, and institutional capacity, expand research and education, and establish fair and transparent natural resource management rules focusing on risk and insurance funds, emergency assistance, and risk recovery.

Regions with higher drought risk in the past (Fig. 1) and future (Supplementary Fig. 7) (West Asia: eastern Turkey, North Iran; Central Asia: southeastern Kazakhstan, southern Uzbekistan, and Turkmenistan; and East Asia: central Mongolia and northern Inner Mongolia) should prioritize measures to increase the feed supply and reserve, risk management by strengthening early warning-action-preparedness and aid/insurance and reduce vulnerability among pastoralists (Table 1). Measures to strengthen institutions in managing rangelands (improve the pasture yield, efficiency use, controlling and reversing degradation, and protecting pastures), livestock (adjust the herd number to match the carrying capacity), and pastoral movement (herd mobility) should be considered in regions where productivity is becoming increasingly vulnerable to drought (e.g., northern Kazakhstan and eastern Mongolia) (Table 1). These measures are especially critical in countries already experiencing low to severe rangeland degradation (e.g., Mongolia: 76.5% of rangelands[30]; Kazakhstan: 66.0% of rangelands[69]; Turkey: 64% of rangelands[70]) as a result of both the combination of increased droughts leading to productivity reduction due to decreased soil moisture together with increased land use (i.e., overpopulated herds above the rangeland carrying capacity)[13,24]. The degraded areas in rangelands could serve as important sinks for greenhouse gas emissions and should be rehabilitated, and climate-friendly agricultural practices should be supported. Moreover, drought-prone regions (eastern Turkey, North Iran, eastern Kazakhstan, Turkmenistan, Uzbekistan, and southwestern Mongolia) are projected to experience drying trends with more hazardous droughts than those during the present period; thus, water crises triggered by climate change will be the most important threat factor[69,71]. Therefore, the protection of water resources, supporting and ensuring the common use of modern water-saving

Table 1 | Synthesis of the existing adaptation measures rooted in the traditional ecological knowledge of pastoralists in the EAR (marked in italics) and potential future measures and practices to adapt pastoralism in the EAR to the increasing vulnerability to droughts and the overall drought risk (refer to Supplementary Table 1 for a list of references)

Objective of the adaptation measures	Measures for adapting to	
	the increasing vulnerability to droughts (V)	the increasing risk of drought impacts (R)
Management improvement	- [P, G] Create and implement local rangeland management plans for user groups - [G, H, R] *Enhance biodiversity by changing grazing techniques (e.g., rotational grazing), facilitating herd mobility, and protecting rangeland* - *Implement restoration* - [P, G, H] Control and reverse rangeland degradation to increase vegetation cover - [G, R] Monitor and control the spread of harmful rodents and insects - [G, P, S, H] Increase water resource protection and management (fencing, harvesting, managing livestock to improve access, and restoring) - [G, H, R] *Adjust the herd number to match the rangeland carrying capacity* - [G, H, R, I] Increase hay harvesting (fencing, fertilizing, seeding, and irrigation) and planting drought-tolerant forage species - [G, S, H] *Protect bushes, shrubs, forest understory, and riparian areas for emergency grazing* - [G, S, S, R, H] Strengthen rangeland fire management and control; enable rapid postfire restoration efforts	- [P, G, R, H, S] Increase the efficiency of rangeland use through revitalization, protection, and forage cultivation - [G, S, H] *Organize herding mobility (short- and long-distance) for rehabilitation of pastures* - [P, G, S, H] Set aside emergency reserves of forage, grazing and/or migration area with livestock shelters and government services (mobile) - [P, G, R] Improve cross-sectoral and/or institutional management coordination to regulate emergency and cross-border movements - [G, S, H, I] *Increase feed reserves by producing and importing hay and fodder* - [G, S, R, H] *Encourage diversification of the livestock composition to utilize the available forage and produce a variety of livestock products* - [G, R, S] Introduce drought-tolerant livestock breeding or crossbreeding and species switching, - [G, R, S, H] Improve veterinary services - [G, R, I] Strengthening early warnings and early actions, forecasting and monitoring of extreme events and forage conditions - [G, S, R, I, H] Enhance early action and disaster preparedness and coordination of actions among all actors from the international to local levels for effective responses
Social transformation	- [G, S, I] Improve the adaptive capacity of herders	- [P, G, S, R, I, H] Encourage livelihood diversification to increase credit access, generate alternative income, and improve market access for pastoral products - [G, S, I, H] Encourage herder groups to form small enterprises and cooperatives for risk management, credit processing and accessing, receiving processing, enterprise development, and marketing training - [P, G, I, S] Provide targeted income assistance to low-income and vulnerable herders - [G, P, I, H] Reduce outmigration by reducing vulnerability and increasing the adaptive capacity
Capacity building	- [G, R, S, I] Improve the knowledge of herders and local officials by teaching traditional and modern advanced methods, rangeland and herd management technologies, and adaptation to climate change - [R, S, I] Monitoring and experimental research on rangeland improvement, opportunities in feed options, and drought-resistant varieties of plant and animal species [G, R, I, S, H] Encourage the traditional adaptive capability (mobility, diversification, storage, etc.)	- [P, G, S] Improve infrastructure with storage capacity and transportation by increasing road and market accessibility levels - [G, R, S, I] Enhance information technology for rural areas and herders to improve dissemination and response networks in a timely manner - [G, R, S, I] Encourage the transfer of technology and capacity development and increase the institutional capacity for hazard response and recovery - [R, I, S, H] Increase research collaboration with herders, livestock organizations, and other pastoralism and rangeland actors - [R, S, I, H] Expand research for integrating traditional and scientific knowledge in adaptation and decision-making processes - [P, G, R, S, I, H] Improve scientific communication between research findings and decision-making processes - [G, R, I] Educate and incentivize pastoralists to adopt greater responsibility for rangeland climate disaster risk, preparedness, and early response - [R, S, I, H] Expand research to assess alternative gendered and equity-based (ethnicity, age, and wealth) approaches to addressing differences in the adaptive capacity within pastoralist communities
Policy reforms	- [P, G, R] Levy rangeland usage fees - [P, G] Establish risk funds to reduce vulnerability	- [P, G] Establish an insurance system for livestock, financial services, savings programs, and cash transfers to increase the effectiveness of drought responses - [P, G] Increase institutional support through policies that address land tenure, fragmentation, and degradation - [G, S, I, H] Increase social protection and create channels for effective emergency assistance to protect vulnerable herders from climate shocks - [P, G, S] Create post-disaster risk recovery programs (emergency response, disaster recovery, and migration, reactive or ex-post adaptation) - [P, G, S, R, I] Increase the participation of herders in decision-making and policy debates, market economies, rangeland management etc. - [P, G, I] Develop adaptation-focused strategic planning and budgeting strategies by identifying socioeconomic issues and financial constraints - [P, G, P, S] Create community and/or group funds (risk management, credit for members, and joint investments in pasture management)

Vulnerability to drought is defined as the difference in rangeland productivity (i.e., the growing season aboveground net primary productivity, ANPP) between nonhazardous and hazardous drought years. Drought risk refers to the potential for adverse effects of hazardous droughts on the ANPP by combining the ANPP vulnerability and the probability of hazardous droughts

Stakeholders: P–Policy-makers;G–government agencies; H–pastoralists; R–research institutions/researchers; I–international organizations; S–other social and economic actors (i.e., mining companies, agricultural enterprises, civil society organizations, and community groups)

techniques, and developing drought-resilient species are important. Overall, a wide range of measures exist for adapting the three regions of the EAR to increasing drought risk and vulnerability levels, and future studies should focus on implementing these measures in a sustainable manner.

Methods

Study area

The study area of the EAR encompasses West, Central, and East Asia, which includes 11 countries (33°−56°N and 25°−128°E) (Fig. 1a and Supplementary Fig. 1). To define the extent of the EAR for pastoralism, we used the

rangelands[72] of the Environmental Systems Research Institute, Inc. (ESRI), land cover map[73] (Fig. 1a) (with excluded grid cells of trees, crops, build-up, and bare lands) as a base map. Then, we combined the base map with grazing lands retrieved from the History database of the Global Environment (HYDE)[73] to define the final EAR (Fig. 1b and Supplementary Fig. 1b, c). We considered grazing lands with fractions above 0.3. In general, climatologically (1985–2014), the annual precipitation (P) in West Asia (490 mm) was greater than that in Central Asia (346 mm) and East Asia (254 mm), with a concentration in April–September (Supplementary Fig. 1a, b). With increasing P and temperature (T), the vegetation greenness (normalized difference vegetation index or NDVI) increases from April on, peaks during regionally different time periods (West Asia: May–June; Central Asia: June–July; and East Asia: July–August) and declines in autumn (September) (Supplementary Fig. 1b). We defined the growing season as April–September to ensure consistency across the EAR. The latitudinal climate pattern (Supplementary Fig. 1c) is a key factor driving the rangeland productivity (as the modeled annual aboveground net primary production (ANPP) and NDVI in April−September ($NDVI_{4-9}$). Favorable rangeland productivity exists in northeastern Central and East Asia and southern West Asia (Supplementary Fig. 1c), which corresponds to the growing season T (T_{4-9}) and P (P_{4-9}) gradients in April–September, with southward and westward decreasing P_{4-9} and increasing T_{4-9} values (Supplementary Fig. 1b).

Probabilistic risk assessment for assessing the vulnerability and drought risk across the EAR

Adapting a probabilistic risk approach (PRA)[45,46], we distinguished environmental (drought, denoted as D in this study) and rangeland ecosystem variables (rangeland productivity: ANNP in this study). Ecosystem variables are expected to be suboptimal when drought values reach levels that constitute hazardous conditions. Numerically, the risk (R) is defined as the expectation of ecosystem loss, i.e., the amount by which the average ecosystem performance is reduced from that under continuously non-hazardous conditions[45,46].

$$R = E\left(\text{rangeland}\middle|D_{non-haz}\right) - E(\text{rangeland}) \quad (1)$$

where E[rangeland] is the overall expected value of the rangeland ecosystem variable (ANPP in this study), and E[rangeland|$D_{non-haz}$] is the expected value of the rangeland ecosystem variable when the drought conditions are nonhazardous ($D_{non-haz}$). Hazardous drought conditions are defined as those where the drought is more extreme than a given threshold, and the probability of occurrence is denoted by $P[D_{haz}]$. Quantitatively, vulnerability (V) is the difference in the ecosystem performance between non-hazardous (favorable) and hazardous (adverse) drought conditions.

$$V = E\left(\text{rangeland}|D_{non-haz}\right) - E(\text{rangeland}|D_{haz}) \quad (2)$$

The risk of the rangeland ecosystem is the product of the probability of hazardous droughts and the vulnerability of the rangeland:

$$R = P[D_{haz}] \times V \quad (3)$$

Equations (1) and (3) are mathematically equivalent, yielding exact risk estimates. A detailed description of PRA implementation is provided in previous studies[45,46].

PRA can be employed to quantify the long-term (30 years in our study) and combined impacts of extreme drought events but cannot be used to evaluate the effect of single events[51,52]. Here, risk analysis was conducted in three consecutive steps. First, we examined $P[D_{haz}]$ during the growing season (April−September) under historical baseline (1985−2014) and future climate changes (2031−2060 and 2071−2100) using the monthly PNI and W_p over the EAR (at a 0.5° × 0.5° spatial resolution). Second, the ANPP was simulated using a process-based vegetation model ORCHIDEE-GM forced by climate observations and GCMs under three SSPs with natural rangeland conditions. Third, we quantified the PRA results for the ANPP in each cell of the grid (0.5° × 0.5°) over the historical baseline (1985–2014) and two future periods (2031–2060 and 2071–2100). The expected values $E\left(\text{rangeland}|D_{non-haz}\right)$ and $E\left(\text{rangeland}\middle|D_{haz}\right)$ were calculated from the frequency distribution of the ecosystem values (ANPP) over the 30-year period. Vulnerabilities and risks were calculated based on Eqs. (2) and (3), respectively. It should be noted that all PRA calculations were performed at the grid level.

We quantified the future changes (in relative terms) in the vulnerability and risk of the rangeland productivity to hazardous droughts by calculating the future changes (Δ) in each value (i.e., the difference between the average of two future periods (2031−2060 and 2070−2100) and the baseline period (1985−2014) by the same GCMs in each grid cell. We obtained the spatial standard deviation (SD) of each region as Δ±SD (%) to assess the climate model uncertainties.

Drought indices

Since precipitation is a proxy indicator of the water available to the coupled human–environment system, the frequency of abnormal precipitation deficits at a certain level of intensity can thus be used to represent the drought hazards for drought-prone ecosystems and society. In this study, to calculate hazardous droughts in each grid cell, we used the PNI[49] (a percentage of the normal precipitation) during April–September, as it provides growing season drought[74] information. The PNI has been commonly used, and its utility has been demonstrated[75]. PNI values <0.8 were designated as dry periods, whereas PNI values ≥1.2 were selected as wet periods. We calculated the PNI using the monthly precipitation obtained from gridded observed and projected climate datasets for 1971–2100 over the EAR by dividing the actual precipitation by the reference precipitation over the time period considered. Here, we considered 1971−2100 as the reference period. Furthermore, we used alternative indicators for droughts using W_p[53]. In this region, this indicator has been used and proven to be a suitable indicator of pasture drought[76]. The root-zone W_p was calculated using soil moisture outputs from the top 50 cm of the soil layer, representing the typical rooting zone in the EAR by ORCHIDEE-GM, which was validated against extensive observations of soil moisture over the EAR. Employing the Weibull distribution of the location data, soil moisture was simulated on a monthly time scale in each grid cell. Moreover, we used the critical growing season SPEI for a 3-month timescale to examine the drought conditions in the future, thereby considering the air temperature and precipitation. The critical growing season was defined as three consecutive months during the growing season with a notable correlation between the SPEI and ANPP as derived from gridded climate data. Here, we used SPEI, spanning the critical growing season months at each grid cell, by identifying the highest correlations between the ANPP and SPEI.

Hazardous drought conditions were defined as PNI ≤−0.7 (moderate to severe droughts), $W_p \le 0.2\%$ (moderate to exceptional droughts), and SPEI ≤−1.0 (moderate to severe droughts) during the growing season (April−September). $P[D_{haz}]$ was calculated as the fraction of each growing season of each 30-year period using PNI ≤0.7, $W_p \le 0.2\%$, and SPEI ≤−1.0. The drought duration can be calculated as the total number of months with PNI ≤0.7 from the beginning to the end of hazardous drought conditions during April−September, and the intensity is defined as the lowest PNI ≤0.7.

Rangeland productivity simulated by a process-based ecosystem model

The daily ANPP and soil moisture were simulated using the ORCHIDEE-GM v3.2 model[65]. ORCHIDEE is a process-based ecosystem model developed for simulating carbon, water, and energy fluxes in ecosystems from the site to the global scales[76–78]. ORCHIDEE-GM was specifically developed for integrating grassland management[47]. In this study, ORCHIDEE-GM was applied over the EAR at a 0.5° × 0.5° spatial resolution for 1901–2100 driven by the observation-based historical climate dataset and downscaled and bias-corrected climate projections of the five GCMs. We considered that all grid cells were covered by C3 grasses (the dominant plant functional type in

the EAR). We used the 12 USDA texture classes[79] provided at a global resolution of 0.08° and upscaled them to the resolution of the atmospheric dataset for the soil texture. Only the dominant texture type for a given grid cell was used at a 0.5° resolution to define the soil hydraulic parameters in the model. To estimate the natural ANPP, we did not consider the grazing pressure. The model was first operated for spin-up purposes without management using the first 10 years of the climate (1901–1910) cycled in a loop and the atmospheric CO_2 concentration for 1900 (296 ppm) until all carbon pools reached equilibrium (long-term net ecosystem exchange = 0 at each grid point). This first spin-up period usually lasts 10,000 years. Then, the model was run over the EAR for 1901–2100, forced by the observed increasing atmospheric CO_2 concentration, variable climate, and variable nitrogen deposition.

The ANNP and soil moisture simulated by ORCHIDEE-GM were validated against the satellite-derived monthly base data, namely, the 0.5° × 0.5° gridded NDVI for April–September ($NDVI_{4-9}$) in 2000–2019, while the simulated soil moisture was evaluated by the observed soil moisture during the growing season at 55 stations in 1978–2015. Generally, at the interannual scale, the observed climate-forced modeled ANPP reasonably agreed with the observed $NDVI_{4-9}$ at 80% of all grid cells ($R > 0.456$, $p < 0.05$) over the EAR in 2000–2019 (Supplementary Fig. 10a). Moreover, the simulated spatiotemporal variations in the ANPP by the five GCMs corresponded well to those in the observed $NDVI_{4-9}$ ($R^2 > 0.85$, $p < 0.05$) (Supplementary Fig. 10b) for 2000–2019. Moreover, the modeled soil moisture in the various soil layers showed satisfactory agreement with the observed soil moisture ($R^2 = 0.83$ in West Asia, $R^2 = 0.90$ in Central Asia, and $R^2 = 0.81$ in East Asia) (Supplementary Fig. 10c) for 1978–2015 for the three regions (corresponding stations). The result suggests that ORCHIDEE-GM could reproduce the spatial and temporal variations in soil moisture and rangeland productivity. However, the model tended to simulate higher soil moisture levels than the observations in higher-productivity areas (northern forest-steppe). Such overestimation probably resulted from location-specific conditions (such as soil properties and topographic features) not explicitly parameterized in the model.

Datasets

Climate data. To examine the changes in climate variables (i.e., T and P) and drought conditions during the growing season, we used two climate datasets in this study, namely, 0.5° × 0.5° grid cell, observed (GSWP3-W5E5[80], 1901−2019) climate data and a downscaled and bias-corrected ISIMIP3b[52] climate dataset covering historical (1971−2014) and future (2015−2100) periods derived from the five GCMs under the three scenarios (SSP1−2.6, SSP3−7.0, and SSP5−8.5).

The GSWP3-W5E5 dataset is based on GSWP3 v1.09[51,81] (version 1.09 of the Global Soil Wetness Project Phase 3) and W5E5 v2.0[51], which are also used as the observational reference dataset for bias adjustment of the climate input data for Inter-Sectoral Impact Model Intercomparison Project 3b-part (ISIMIP3b)[82]. W5E5 v2.0 combines WFDE5 v2.0 (WATCH Forcing Data methodology applied to European Reanalysis, ERA5) data over land[50] with data from the latest version of the ERA5[83] over the ocean. Since W5E5 v2.0 only covers the 1979 to 2019 period, it was extended backward in time to 1901. To this end, the GSWP3 dataset, bias-adjusted to W5E5 v2.0, reduces any discontinuities during the 1978–1979 transition. The method used for bias adjustment was ISIMIP3BASD v2.5[52,82]. The GSWP3 dataset is a dynamically downscaled and bias-adjusted version of the Twentieth Century Reanalysis version 2 (20CRv2) product[84]. The GSWP3-W5E5 data consist of the following ten meteorological variables: 2-m temperature, 2-m maximum and minimum temperatures, total precipitation, specific humidity, downward solar radiation flux, downward longwave radiation flux, pressure, and zonal and meridional components of the wind speed.

ISIMIP3b bias adjustment and statistical downscaling of the CMIP6 output using ISIMIP3BASD v2.5.0 and W5E5 v2.0 are described in the ISIMIP3b bias adjustment fact sheet (https://www.isimip.org/documents/413/ISIMIP3b_bias_adjustment_fact_sheet_Gnsz7CO.pdf). The five GCMs selected for bias adjustment are suitable representatives of the entire CMIP6 ensemble, as they include three models with low climate sensitivity (GFDL-ESM4, MPI-ESM1-2-HR, and MRI-ESM2-0) and two models with high climate sensitivity (IPSL-CM6A-LR and UKESM1-0-LL).

Ground and satellite observations

Regarding model validation, we used satellite-derived monthly gridded (0.5° × 0.5°) Moderate Resolution Imaging Spectroradiometer (MODIS) $NDVI_{4-9}$ data, which were derived from the 16-d 0.05° × 0.05° spatial resolution MOD13C1 dataset for 2000–2020, obtained from the NASA Land Processes Distributed Active Archive Center (LP DAAC)[85]. To validate the modeled soil moisture in the various soil layers, we used daily and 10-day ground-based measurements of soil moisture in grass fields at stations for 1978–2015, which were collected from the top 50 cm of the soil layer, representing the typical rooting zone in the EAR[86,87]. The locations of the sampling stations are shown in Supplementary Fig. 10a. In West Asia, a total of 15 stations across Turkey[88] for the 0–10 cm soil layer in April–September of the 2008–2016 period, 17 stations in Central Asia from International soil moisture datasets[89] (Kazakhstan, Uzbekistan, Tajikistan, and Kyrgyzstan) for the 0–5 and 0–10 cm soil layers in 1978–1985 and 2001–2011, and 22 stations in East Asia (20 stations in Mongolia[86] for the 0–50 cm soil layer from 1986–2005 and 2 stations in Inner Mongolia[87] for the 0–5 cm depth in 2005–2015), were used for obtaining soil moisture validations. The soil moisture measurements in Turkey and Inner Mongolia were conducted by soil moisture sensors on a daily basis throughout the year, while in the other countries, the soil moisture measurements were conducted on the 8th, 18th, and 28th of each month during the warm season (April–October) using the gravimetric method.

Data availability

The bias-corrected climate model outputs are available at https://data.isimip.org/search/tree/ISIMIP3b/InputData/climate/. The data which support the findings of this study are available in a public repository with a DOI (doi: 10.6084/m9.figshare.25224899).

Code availability

The source code for ORCHIDEE-GM v3.2 is available at https://doi.org/10.14768/ 20190319001.1.

Received: 11 August 2023; Accepted: 13 March 2024;
Published online: 29 March 2024

References

1. Olson, D. M. et al. Terrestrial ecoregions of the world: a new map of life on earth. *Bioscience* **51**, 933–938 (2001).
2. Boone, R. B. et al. Climate change impacts on selected global rangeland ecosystem services. *Glob. Chang. Biol.* **24**, 1382–1393 (2018).
3. Thornton, P. K. et al. The impacts of climate change on livestock and livestock systems in developing countries: a review of what we know and what we need to know. *Agric. Syst.* **101**, 113–127 (2009).
4. Godde, C. M. et al. Impacts of climate change on the livestock food supply chain; a review of the evidence. *Glob. Food Sec.* **28**, 100488 (2021).
5. Scoones, I. et al. Pastoralism and development: fifty years of dynamic change. *IDS Bull*. **51**, (2020).
6. Kerven, C., Robinson, S. & Behnke, R. Pastoralism at scale on the Kazakh rangelands: from clans to workers to ranchers. *Front. Sustain. Food Syst.* **4**, 590401 (2021).
7. Neely, C., Bunning, S. & Wilkes, A. (eds). *Review of Evidence on Drylands Pastoral Systems and Climate Change. Implications and Opportunities for Mitigation and Adaptation* (Food and Agriculture Organization, 2009).
8. Zinsstag, J. et al. A vision for the future of pastoralism. *Rev. Sci. Tech.* **35**, 693–699 (2016).

9. Honeychurch, W. et al. The earliest herders of East Asia: examining Afanasievo entry to Central Mongolia. *Archaeol. Res. Asia* **26**, 100264 (2021).
10. FAO (Food and Agriculture Organization). FAOSTAT land, inputs and sustainability, livestock patterns. http://www.fao.org/faostat/en/#data/EK (2023).
11. Sloat, L. L. et al. Increasing importance of precipitation variability on global livestock grazing lands. *Nat. Clim. Chang* **8**, 214–218 (2018).
12. Liu, D. et al. Increasing climatic sensitivity of global grassland vegetation biomass and species diversity correlates with water availability. *N. Phytol.* **230**, 1761–1771 (2021).
13. Nandintsetseg, B. et al. Risk and vulnerability of Mongolian grasslands under climate change. *Environ. Res. Lett.* **16**, 034035 (2021).
14. Mirzabaev, A. et al. Rangelands of Central Asia: challenges and opportunities. *J. Arid Land* **8**, 93–108 (2016).
15. Berkes, F., Colding, J. & Folke, C. Rediscovery of traditional ecological knowledge as adaptive management. *Ecol. Appl.* **10**, 1251–1262 (2000).
16. Herrero, M. et al. Climate change and pastoralism: Impacts, consequences and adaptation. *Rev. Sci. Tech.* **35**, 417–433 (2016).
17. Thevenin, M. Kurdish transhumance: pastoral practices in South-east Turkey. *Pastoralism* **1**, 23 (2011).
18. Kakinuma, K. et al. Herding strategies during a drought vary at multiple scales in Mongolian rangeland. *J. Arid Environ.* **109**, 88–91 (2014).
19. Fernandez-Gimenez, M. E. The role of Mongolian nomadic pastoralists' ecological knowledge in rangeland management. *Ecol. Appl.* **10**, 1318–1326 (2000).
20. Mearns, R. Sustaining livelihoods on Mongolia's pastoral commons: Insights from a participatory poverty assessment. *Dev. Change* **35**, 107–139 (2004).
21. Dubovyk, O. et al. Drought hazard in Kazakhstan in 2000–2016: a remote sensing perspective. *Environ. Monit. Assess.* **191**, 510 (2019).
22. Groisman, P. et al. Dryland belt of Northern Eurasia: contemporary environmental changes and their consequences. *Environ. Res. Lett.* **13**, 115008 (2018).
23. Reyer, C. P. O. et al. Climate change impacts in Central Asia and their implications for development. *Reg. Environ. Change* **17**, 1639–1650 (2017).
24. Nandintsetseg, B., Shinoda, M. & Erdenetsetseg, B. Contributions of multiple climate hazards and overgrazing to the 2009/2010 winter disaster in Mongolia. *Nat. Haz.* **92**, 109–126 (2018).
25. Sekercioglu, C. H. et al. Turkey's globally important biodiversity in crisis. *Biol. Conser.* **144**, 2752–2769 (2011).
26. Alsafadi, K. et al. An evapotranspiration deficit-based drought index to detect variability of terrestrial carbon productivity in the Middle East. *Environ. Res. Lett.* **17**, 014051 (2022).
27. Liu, Y. et al. Concurrent and lagged effects of drought on grassland net primary productivity: a case study in Xinjiang, China. *Front. Ecol. Evol.* **11**, 1131175 (2023).
28. Deng, H., Yin, Y. & Han, X. Vulnerability of vegetation activities to drought in Central Asia. *Environ. Res. Lett.* **15**, 084005 (2020).
29. Ellis, J. & Lee, R. Y. *Prospects for Pastoralism in Kazakhstan and Turkmenistan from State Farms to Private Flocks (ed. Kervin, C.)* 52–71 (RoutledgeCurzon, 2003).
30. NAMEM-MEGDT. *National Report on the Rangeland Health of Mongolia*. https://en.greenmongolia.mn/post/103686 (2015).
31. Nandintsetseg, B., Shinoda, M., Du, C. & Munkhjargal, E. Cold-season disasters on the Eurasian steppes: climate-driven or man-made. *Sci. Rep.* **8**, 14769 (2018).
32. Du, C. et al. Mongolian herders' vulnerability to dzud: a study of record livestock mortality levels during the severe 2009/2010 winter. *Nat. Haz.* **92**, 3–17 (2017).
33. IOM. *Mongolia: Internal Migration Study* (International Organization for Migration, 2018).
34. Mayer, B. *Climate Change in the Asia-Pacific Region* (ed. Filho, L. W.) 191–204 (Springer, 2015).
35. Rechkemmer, A. et al. A complex social-ecological disaster: environmentally induced forced migration. *Disaster Health* **3**, 112–120 (2016).
36. Groppo, V. & Kraehnert, K. Extreme weather events and child height: evidence from Mongolia. *World Dev.* **86**, 59–78 (2016).
37. Otani, S. et al. Assessment of the effects of severe winter disasters (Dzud) on public health in Mongolia on the basis of loss of livestock. *Disaster Med. Public Health Prep.* **10**, 549–552 (2016).
38. Balting, D. F., AghaKouchak, A., Lohmann, G. & Ionita, M. Northern hemisphere drought risk in a warming climate. *NPJ Clim. Atmos. Sci.* **4**, 61 (2021).
39. IPCC. *Climate Change 2022: Impacts, Adaptation, and Vulnerability. Contribution of Working Group II to the Sixth Assessment Report of the Intergovernmental Panel on Climate Change*. *Climate Change 2022 – Impacts, Adaptation and Vulnerability* (Cambridge Univ. Press, 2022).
40. UN SDGs. United Nations, sustainable development knowledge platform, sustainable development goals. https://sdgs.un.org/goals (2023).
41. IPCC. *Climate Change 2014: Impacts, Adaptation, and Vulnerability. Part A: Global and Sectoral Aspects* (Cambridge Univ. Press, 2014).
42. UN DHA. *Internationally Agreed Glossary of Basic Terms Related to Disaster Management* (DHA, 1992).
43. Aven, T. Risk assessment and risk management: review of recent advances on their foundation. *Eur. J. Oper. Res.* **253**, 1–13 (2016).
44. Hope, B. K. Generating probabilistic spatially-explicit individual risk assessments. *Risk Anal.* **20**, 573–590 (2000).
45. Van Oijen, M. et al. Impact of droughts on the carbon cycle in European vegetation: a probabilistic risk analysis using six vegetation models. *Biogeoscience* **11**, 6357–6375 (2014).
46. Van Oijen, M. et al. A novel probabilistic risk analysis to determine the vulnerability of ecosystems to extreme climatic events. *Environ. Res. Lett.* **8**, 015032 (2013).
47. Chang, J. F. et al. Incorporating grassland management in ORCHIDEE: model description and evaluation at 11 eddy-covariance sites in Europe. *Geosci. Model Dev.* **6**, 2165–2181 (2013).
48. Chang, J. et al. Future productivity and phenology changes in European grasslands for different warming levels: implications for grassland management and carbon balance. *Carbon Balance Manag.* **12**, 11 (2017).
49. Salehnia, N. et al. Estimation of meteorological drought indices based on AgMERRA precipitation data and station-observed precipitation data. *J. Arid Land* **9**, 797–809 (2017).
50. Cucchi, M. et al. WFDE5: bias adjusted ERA5 reanalysis data for impact studies Earth system science data discussions. *Earth Syst. Sci. Data* **12**, 2097–2120 (2020).
51. Kim, H. *Global Soil Wetness Project Phase 3 Atmospheric Boundary Conditions* (Experiment 1). (Data Integration and Analysis System (DIAS), 2017).
52. Lange, S., Quesada-Chacón, D. & Büchner, M. Secondary ISIMIP3b bias-adjusted atmospheric climate input data (v1.2). *ISIMIP Repository* https://doi.org/10.48364/ISIMIP.581124.2 (2023).
53. CPC (Climate Prediction Center). National Weather Service. https://www.weather.gov/riw/drought (2023).
54. Vicente-Serrano, S. M., Beguería, S. & López-Moreno, J. I. A multiscalar drought index sensitive to global warming: the standardized precipitation evapotranspiration index. *J. Clim.* **23**, 1696–1718 (2010).
55. Hua, L., Zhao, T. & Zhong, L. Future changes in drought over Central Asia under CMIP6 forcing scenarios. *J. Hydrol. Reg. Stud.* **43**, 101191 (2022).
56. Wang, T. et al. Global data assessment and analysis of drought characteristics based on CMIP6. *J. Hydrol.* **596**, 126091 (2021).
57. Zhao, T. & Dai, A. CMIP6 model-projected hydroclimatic and drought changes and their causes in the twenty-first century. *J. Clim.* **35**, 897–921 (2022).

58. Babaousmail, H. et al. Future changes in mean and extreme precipitation over the Mediterranean and Sahara regions using bias-corrected CMIP6 models. *Inter. J. Climatol.* **42**, 7280–7297 (2022).
59. Ainsworth, E. A. & Long, S. P. What have we learned from 15 years of free-air CO2 enrichment (FACE)? A meta-analytic review of the responses of photosynthesis, canopy properties and plant production to rising CO2. *N. Phytol.* **165**, 351–372 (2005).
60. Shi, H. et al. Saturation of global terrestrial carbon sink under a high warming scenario. *Glob. Biogeochem. Cycles* **35**, e2020GB006800 (2021).
61. Swann, A. L. S., Hoffman, F. M., Koven, C. D. & Randerson, J. T. Plant responses to increasing CO2 reduce estimates of climate impacts on drought severity. *Proc. Natl Acad. Sci. USA* **113**, 10019–10024 (2016).
62. Pan, Y. et al. Contrasting responses of woody and grassland ecosystems to increased CO2 as water supply varies. *Nat. Ecol. Evol.* **6**, 315–323 (2022).
63. Chang, J. et al. Modeled changes in potential grassland productivity and in grass-fed ruminant livestock density in Europe over 1961-2010. *PLoS ONE* **10**, e0127554 (2015).
64. Chang, J. et al. Combining livestock production information in a process-based vegetation model to reconstruct the history of grassland management. *Biogeoscience* **13**, 3757–3776 (2016).
65. Chang, J. et al. Climate warming from managed grasslands cancels the cooling effect of carbon sinks in sparsely grazed and natural grasslands. *Nat. Commun.* **12**, 118 (2021).
66. Ito, A. et al. Photosynthetic productivity and its efficiencies in ISIMIP2a biome models: Benchmarking for impact assessment studies. *Environ. Res. Lett.* **12**, 085001 (2017).
67. Chang, J. et al. Benchmarking carbon fluxes of the ISIMIP2a biome models. *Environ. Res. Lett.* **12**, 045002 (2017).
68. Ferret, C. Mobile pastoralism a century apart: continuity and change in south-eastern Kazakhstan, 1910 and 2012. *Centr. Asian Surv.* **37**, 503–525 (2018).
69. FAO (Food and Agriculture Organization). *Drought Characteristics and Management in Central Asia and Turkey* (FAO, 2017).
70. Ministry of Forestry and Water Affairs. *National Strategy and Action Plan to Combat Desertification* (2015).
71. ADB. *Making Grasslands Sustainable in Mongolia Herders' Livelihoods and Climate Change* (Asian Development Bank, 2014).
72. ESRI. Esri. Sentinel-2 10m Land Use/Land Cover Time Series. *Esri. Sentinel-2 10 m Land Use/Land Cover Time Series*. https://www.esri.com/partners/impact-observatory-a2T5x0000084pJXEAY/sentinel-2-10m-land--a2d5x000005jw9NAAQ (2023).
73. Goldewijk, K. K., Beusen, A., Doelman, J. & Stehfest, E. Anthropogenic land use estimates for the Holocene; HYDE 3.2. *Earth Sys. Sci. Data* **9**, 927–953 (2017).
74. Nandintsetseg, B. & Shinoda, M. Assessment of drought frequency, duration, and severity and its impact on pasture production in Mongolia. *Nat. Haz.* **66**, 995–1008 (2013).
75. Cancelliere, A., Mauro, G., Di, Bonaccorso, B. & Rossi, G. Drought forecasting using the standardized precipitation index. *Water Res. Manag.* **21**, 801–819 (2007).
76. Ciais, P. et al. Europe-wide reduction in primary productivity caused by the heat and drought in 2003. *Nature* **437**, 529–533 (2005).
77. Krinner, G. et al. A dynamic global vegetation model for studies of the coupled atmosphere-biosphere system. *Glob. Biogeochem. Cycles* **19**, GB1015 (2005).
78. Piao, S. et al. Growing season extension and its impact on terrestrial carbon cycle in the Northern Hemisphere over the past 2 decades. *Glob. Biogeochem. Cycles* **21**, GB3018 (2007).
79. Reynolds, C. A., Jackson, T. J. & Rawls, W. J. Estimating soil water-holding capacities by linking the Food and Agriculture Organization soil map of the world with global pedon databases and continuous pedotransfer functions. *Wat. Res. Res.* **36**, 3653–3662 (2000).
80. Mengel, M., Treu, S., Lange, S. & Frieler, K. ATTRICI v1.1 – counterfactual climate for impact attribution. *Geosci. Model Dev.* **14**, 5269–5284 (2021).
81. Dirmeyer, P. A. et al. GSWP-2: multimodel analysis and implications for our perception of the land surface. *Bull. Am. Meteorol. Soc.* **87**, 1381–1398 (2006).
82. Lange, S. Trend-preserving bias adjustment and statistical downscaling with ISIMIP3BASD (v1.0). *Geosci. Model Dev.* **12**, 3055–3070 (2019).
83. Hersbach, H. et al. The ERA5 global reanalysis. *Q. J. R. Meteorol. Soc.* **146**, 1999–2049 (2020).
84. Compo, G. P. et al. The twentieth century reanalysis project. *Q. J. R. Meteorol. Soc.* **137**, 1–28 (2011).
85. Didan, K. & Huete, A. MOD13C2 MODIS/Terra Vegetation Indices Monthly L3 Global 0.05Deg CMG V006. NASA EOSDIS Land Processes DAAC https://lpdaac.usgs.gov/products/mod13c2v006/ (2015).
86. Nandintsetseg, B. & Shinoda, M. Seasonal change of soil moisture in Mongolia: Its climatology and modelling. *Int. J. Climatol.* **31**, 1143–1152 (2011).
87. Yong, M. et al. Impacts of land surface conditions and land use on dust events in the inner Mongolian Grasslands, China. *Front. Ecol. Evol.* **9**, 664900 (2021).
88. Bulut, B. et al. Evaluation of remotely-sensed and model-based soil moisture products according to different soil type, vegetation cover and climate regime using station-based observations over Turkey. *Remote Sens.* **11**, 1875 (2019).
89. Dorigo, W. et al. The international soil moisture network: serving Earth system science for over a decade. *Hydrol. Earth Sys. Sci.* **25**, 5749–5804 (2021).

Acknowledgements

This study was supported by 2236 Co-Funded Brain Circulation Scheme 2 (CoCirculation2) of TÜBİTAK and European Commission Horizon 2020 Marie Skłodowska-Curie Actions [Grant No. 121C054] and the National Natural Science Foundation of China [Grant No. 32222053]. The funder played no role in the study design, data collection, analysis and interpretation of data, or the writing of this manuscript. The authors are grateful to Dr. Tugrul Yilmaz, M. and Dr. Yong Mei for sharing soil moisture observations in Turkey and Inner Mongolia.

Author contributions

B.N. and J.C. contributed equally to this work. B.N. and J.C. designed the study with C.P.O.R. and performed the research; B.N., J.C., K.K., and J.D. analyzed the data; B.N. and J.C. wrote the paper with input from C.P.O.R. and comments and edits from all authors. All authors read and approved the final manuscript.

Competing interests

The authors declare no competing interests.

Additional information

Supplementary information The online version contains supplementary material available at https://doi.org/10.1038/s41612-024-00624-2.

Correspondence and requests for materials should be addressed to Banzragch Nandintsetseg or Jinfeng Chang.